

Electrochemical Analysis of Direct Methanol Fuel Cells for Low Temperature Operation

V. Baglio*, A. Di Blasi, E. Modica, P. Cretì, V. Antonucci, A. S. Aricò

CNR-ITAE, Via Salita S. Lucia sopra Contesse, 5 – 98126 Messina, Italy

*E-mail: baglio@itae.cnr.it; tel. +39090624237; fax +39090624247

Received: 8 May 2006 / Accepted: 24 May 2006 / Published: 27 May 2006

The electrochemical behaviour of Direct Methanol Fuel Cells (DMFCs) was investigated at low temperatures (30°C-60°C). An 85 wt% Pt-Ru (1:1 a/o)/C anode catalyst and a 60 wt% Pt/C cathode catalyst were in-house prepared and characterised. The influence of noble metal loading on the performance of a DMFC based on these catalysts was studied by steady-state polarisation measurements. The DMFC maximum power density increased linearly from 30 to 75 mW·cm⁻² at 60°C passing from 1 to 5 mg·cm⁻² Pt loading in both electrodes. By further increasing the Pt loading at 10 mg·cm⁻² only a slight increase of power density was recorded (81 mW·cm⁻²).

Keywords: Direct Methanol Fuel Cells, Pt loading, Low temperature, Portable application.

1.INTRODUCTION

One of the most promising applications of Direct Methanol Fuel Cells (DMFCs) presently concerns with the field of portable power sources [1-4]. In this regard, increasing interest is devoted towards the miniaturisation of these fuel cell devices in order to replace the current Li-ion batteries. Theoretically, methanol has a superior specific energy density (6000 Wh/kg) in comparison with the best rechargeable battery, lithium polymer and lithium ion polymer (600 Wh/kg) systems. This means longer conversation times using mobile phones, longer times for use of laptop computers and more power available on these devices to support consumer demand. Another significant advantage of the DMFC over the rechargeable battery is its potential for instantaneous refuelling. These significant advantages make DMFCs an exciting development in the portable electronic devices market [5-7]. Unfortunately, DMFC operation at low temperatures requires a high noble metal loading to enhance the kinetics of the methanol electro-oxidation reaction and counteract the poisoning effects at the cathode due to the methanol cross-over [5, 8, 9].

In order to reduce ohmic drop, mass transport and manufacturing problems deriving by the use of thick electrodes, the present DMFC catalysts for low temperature applications are usually unsupported Pt and Pt-Ru alloys [10-12]. Yet, the presence of catalyst agglomeration effects in unsupported catalysts significantly limits their utilisation in polymer electrolyte fuel cell systems. In this work, an 85% Pt-Ru (1:1 a/o) alloy supported on Vulcan XC-72 and a 60% Pt/Vulcan XC-72 were in-house prepared and utilised in DMFCs as anode and cathode catalysts, respectively. These carbon supported catalysts associate high metal surface area to a suitable concentration of the active phase that allows to maintain a low electrode thickness. The influence of noble metal loading on the performance of a DMFC operating at low temperatures (30-60°C) has been investigated. This effect has been correlated to catalyst utilisation and electro-catalytic activity at the different temperatures.

2. EXPERIMENTAL

An 85% Pt-Ru (1:1 a/o)/Vulcan XC-72 and a 60% Pt/Vulcan XC-72 were in-house prepared by using a sulphite complex route [13]. The preparation procedure involved three main steps: (i) synthesis of the Pt and Ru sulphite precursors, (ii) decomposition of the precursors by H₂O₂ into colloidal amorphous oxides, (iii) gas phase reduction in a hydrogen stream to form metallic phases. A description of the preparation procedure has been reported elsewhere [14]. X-ray diffraction powder (XRD) patterns of the anode and cathode catalysts were obtained on a Philips X'Pert X-ray diffractometer using a CuK_α-source. TEM analysis was carried out by a Philips CM12 microscope. The electrodes were prepared according to the procedure described in a previous paper [12]; they consisted of carbon cloth, diffusion and catalytic layers. An 85% Pt-Ru alloy (1:1)/C catalyst was employed at the anode; whereas, a 60% Pt/C catalyst was utilized for cathode fabrication. The catalysts were intimately mixed with Nafion ionomer (85 wt% catalyst, 15 wt% Nafion ionomer on a dry basis) by ultrasonic treatment. Pt loadings ranging between 1 and 10 mg cm⁻² were used for both anode and cathode. A Nafion 117 membrane was used as electrolyte. Membrane-electrode assemblies (MEAs) were formed by a hot-pressing procedure [12] and subsequently installed in a fuel cell test fixture of 5 cm² active area. This latter was connected to a test station including an HP6060B electronic load or to an EG&G electrochemical apparatus consisting of a PAR 273A Potentiostat/Galvanostat and a 20A Current Booster. For single cell polarization experiments, aqueous methanol (1M) was pre-heated at the same temperature of the cell and fed to the anode chamber of the DMFC through a peristaltic pump; dry air, pre-heated at the same temperature of the cell, was fed to the cathode. Atmospheric pressure in the anode and cathode compartments was used for all the experiments. Reactant flow rates were 2 ml min⁻¹ and 350 ml min⁻¹ for methanol/water mixture and air stream, respectively. Single cell performances were investigated by steady-state galvanostatic polarization measurements. In-situ stripping voltammetry of adsorbed methanolic residues at the anode under normal operation (1 M CH₃OH feed with a flow of 2 ml min⁻¹) was carried out at various temperatures under DMFC configuration following a procedure previously reported [14].

3. RESULTS AND DISCUSSION

X-ray diffraction analysis (Figure 1) shows for both the cathode and anode catalysts the diffraction peaks of the fcc structure typical of Pt and Pt-Ru alloy, respectively. Due to the high concentration of noble metals supported on carbon black, only a slight X-ray scattering for graphitic carbon is observed at about $2\theta \cong 25^\circ$. A shift to higher Bragg angles and an increase of peak broadening is observed for the Pt-Ru catalyst with respect to pure Pt, indicating a decrease of lattice parameters and average particle size, respectively. This latter is about 21 Å for the Pt-Ru alloy catalyst and 37 Å for the Pt catalyst, as calculated by the Sherrer equation.

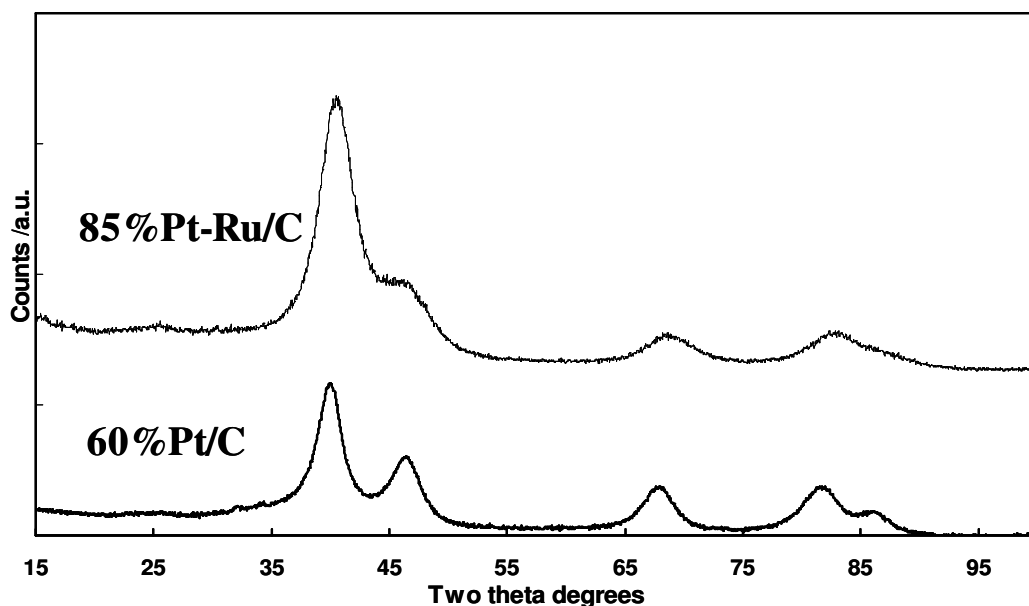
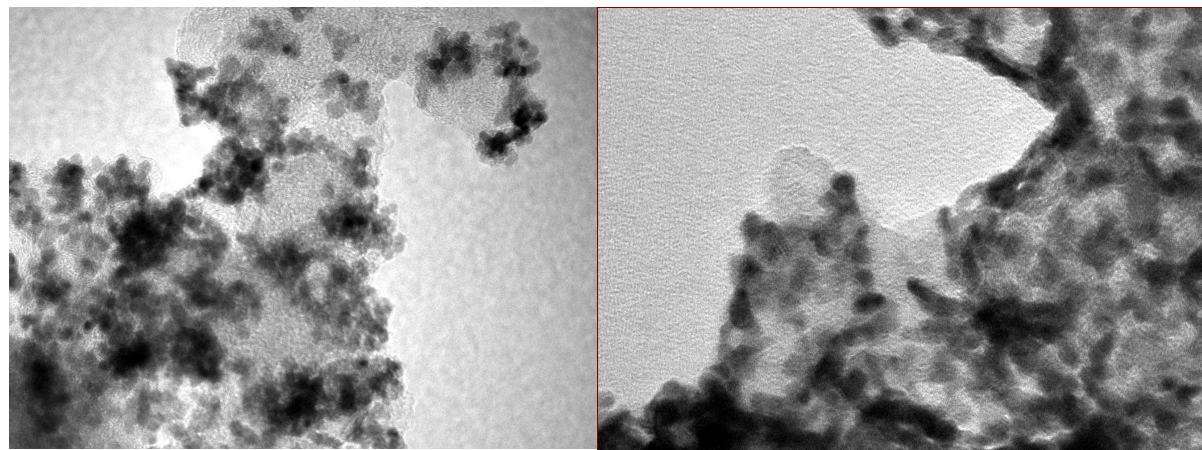


Figure 1. XRD patterns of 85% Pt-Ru/C and 60% Pt/C catalysts.

TEM observation of the two catalysts (Figure 2) shows a good dispersion of the metal particles on the support, even if some particle agglomerations due to the high concentration of metal on carbon support are observed.

The influence of noble metal loading on the performance of a DMFC operating at low temperatures (30-60°C) was first investigated by steady-state polarization measurements, feeding 1M MeOH solution to the anode and dry air to the cathode side under atmospheric pressure. Accordingly, a Pt content comprised between 1 and 10 mg·cm⁻² was used in these experiments. Figure 3 shows the polarisation and power density curves obtained at 30°C for the different cells equipped with the various Pt loadings. In these experiments the same Pt loading was both at the anode and cathode. At 30°C the increase of power density passing from 3.5 to 5 mg·cm⁻² Pt loading is quite significant. Less significant is the increase passing from 5 to 10 mg·cm⁻². Accordingly, 5 mg·cm⁻² would be a suitable Pt loading for this application. This is confirmed by successive experiments at different temperatures. Figure 4 shows the polarization and power density curves recorded at 60°C in the same conditions. The

voltage losses decrease in the overall range of current densities as the Pt loading is increased from 1 to 5 mg·cm⁻²; whereas, in the case of 10 mg·cm⁻², significant mass transfer limitations are observed at high currents. However, at 0.5 V, the current density for the cell equipped with 10 mg·cm⁻² is higher



(a)

(b)

Figure 2. Transmission electron micrographs of (a) 85% Pt-Ru/C and (b) 60% Pt/C catalysts.

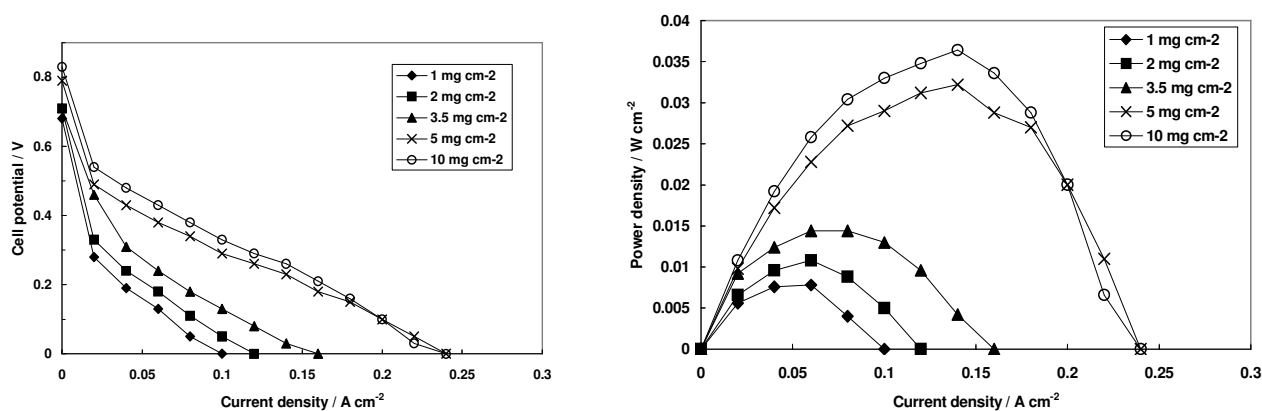


Figure 3. Polarisation and power density curves at 30°C for DMFCs equipped with 85% Pt-Ru/C and 60% Pt/C catalysts at various Pt loadings under atmospheric pressure

than that recorded with 5 mg·cm⁻² Pt content. A progressive increase of performance is recorded passing from 1 to 5 mg·cm⁻²; the maximum power density increases from 30 to 75 mW·cm⁻² at 60°C and atmospheric pressure. By further increasing the Pt loading at 10 mg·cm⁻² only a slight increase of power density was recorded (81 mW·cm⁻²). The performance is still better at very low current density in the activation region, but due to a decrease of the catalyst utilization (see below) the performance of the cell based on electrodes containing 10 mg Pt cm⁻² is lower than that expected.

In-situ stripping voltammetry analysis of the anode catalyst (Figure 5) shows that the stripping charges associated with the adsorbed methanolic residues increase as a function of the Pt loading, but the

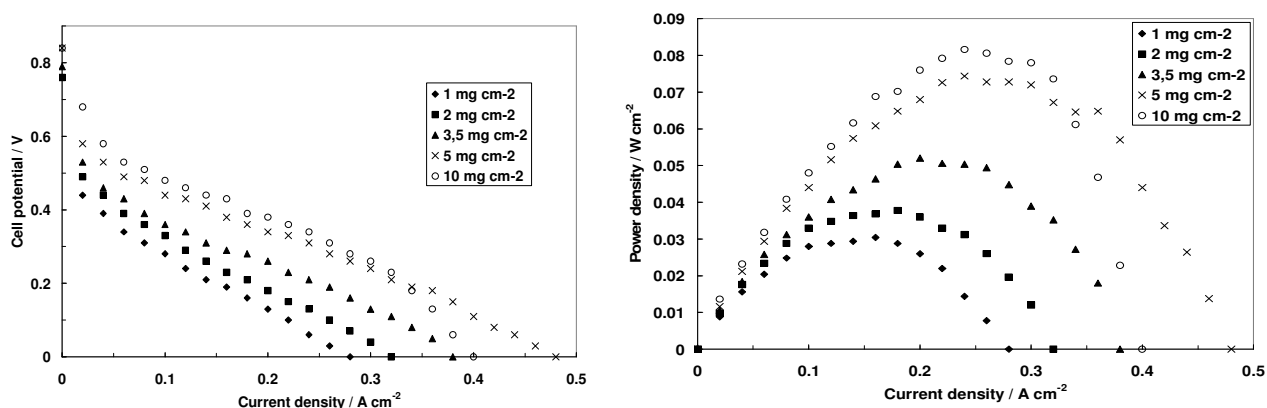


Figure 4. Polarisation and power density curves at 60°C for DMFCs equipped with 85% Pt-Ru/C and 60% Pt/C catalysts at various Pt loadings under atmospheric pressure.

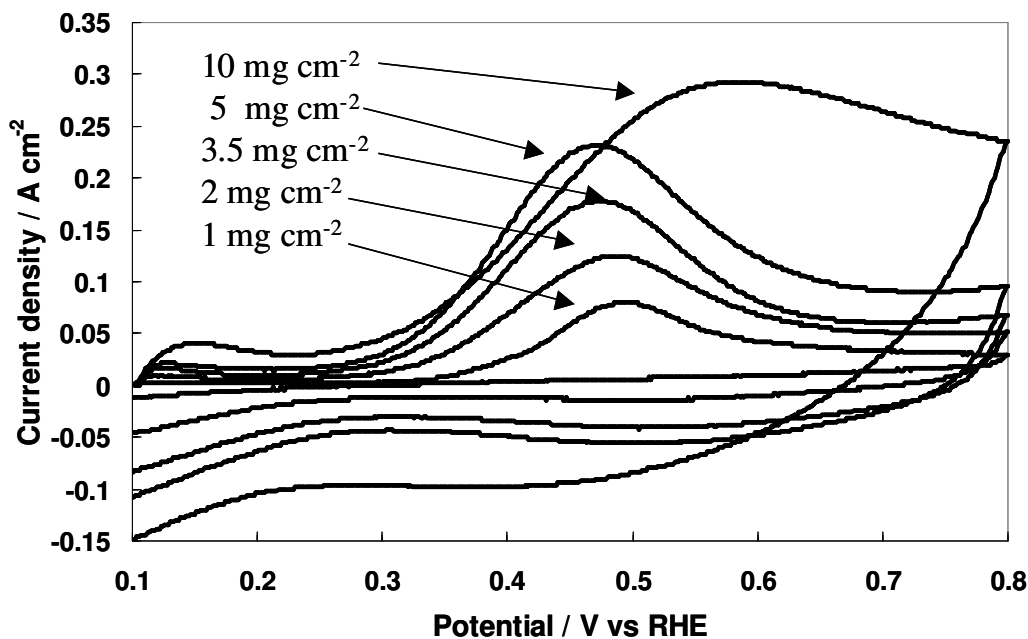


Figure 5. In-situ adsorbed methanolic residues stripping voltammetry at 85% Pt-Ru/C | Nafion 117 membrane interface in the presence of various Pt loadings at 60°C under the DMFC configuration.

electrochemical active surface area decreases as the Pt content is increased to 10 mg·cm⁻². In Figure 6 the maximum power density and the electrochemical surface area are plotted as a function of Pt loading. It is evident from this analysis that the performance of the DMFC does not increase significantly passing from 5 to 10 mg·cm⁻² Pt loading on both electrodes at 60 °C (Figure 6a). Correspondingly, the catalyst utilization decreases significantly when the Pt loading is increased from 5 to 10 mg·cm⁻² (Figure 6b). This can be explained by considering that the three-phase reaction zone does not extend to the overall electrode thickness but it is limited to the electrode – electrolyte interface. Methanol adsorption at 0.1 V, thus, occurs especially close to the electrode-electrolyte

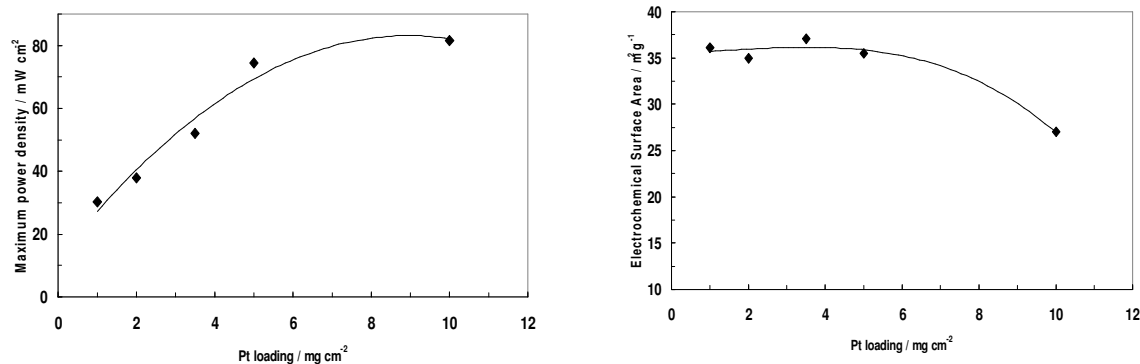


Figure 6. Variation of (a) maximum power density and (b) electrochemical surface area as a function of Pt loading in DMFCs equipped with 85% Pt-Ru/C and 60% Pt/C catalysts. Cell temperature: 60°C

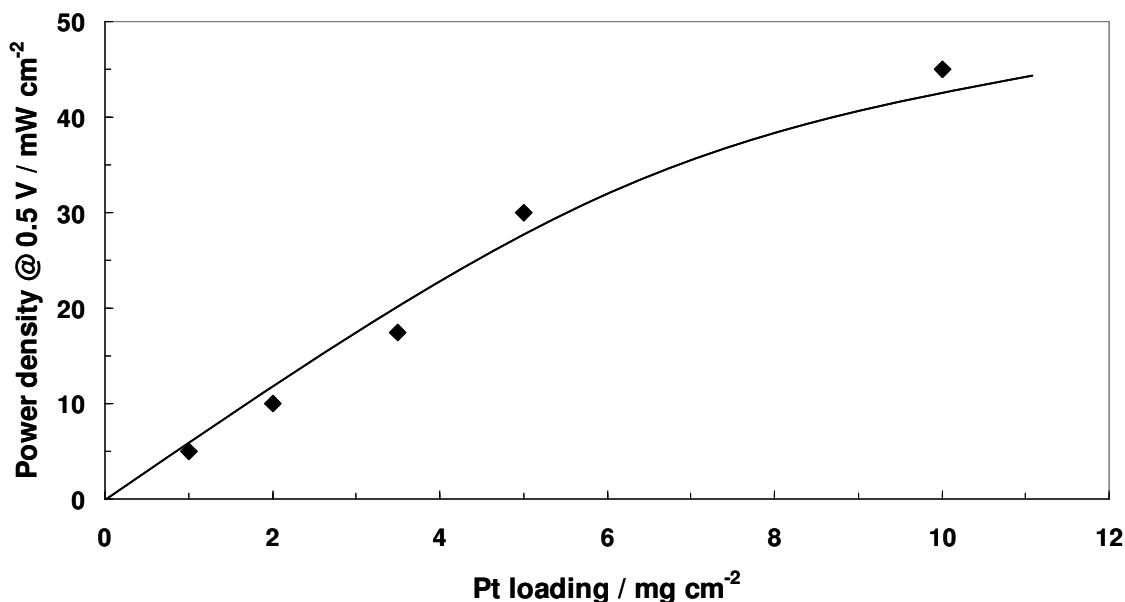


Figure 7. Variation of power density at 0.5 V as a function of Pt loading in DMFCs equipped with 85% Pt-Ru/C and 60% Pt/C catalysts. Cell temperature: 60°C

interface. However, in the activation controlled region the performance for the 10 mg·cm⁻² Pt loading cell is still better than the 5 mg·cm⁻² Pt-based cell, since the decrease of the Pt utilization is less than 50 %. At high current density, mass transfer limitations are also observed in the case of the 10 mg·cm⁻² Pt cell, as above discussed. The mass transfer constraints are probably due to the large electrode thickness. These effects are also probably reflected in the stripping voltammogram of the anode (Figure 5). Accordingly, 5 mg·cm⁻² Pt loading seems to be the optimal content in terms of maximum power density for low temperature (30-60°C) DMFCs. Similar behaviour is observed for the power density at 0.5 V as a function of Pt loading (Figure 7).

Figure 8 shows the influence of temperature on the single cell polarisation and power density

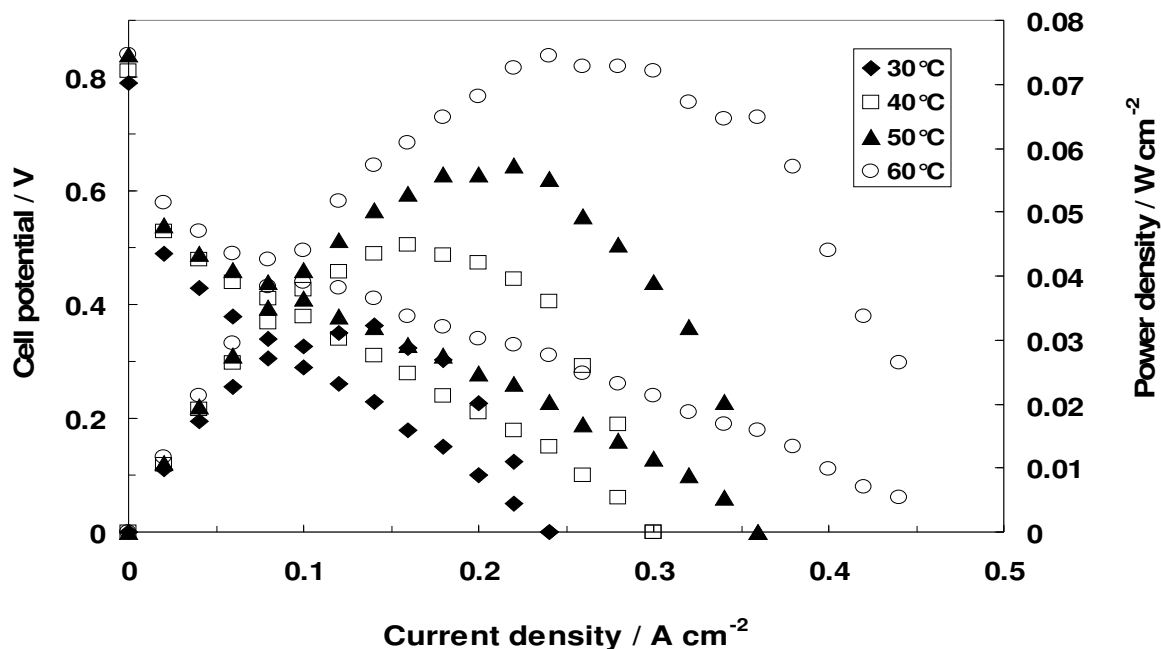


Figure 8. Polarisation and power density curves at various temperatures for DMFCs equipped with 85% Pt-Ru/C and 60% Pt/C catalysts with 5 mg cm⁻² Pt loading under atmospheric pressure.

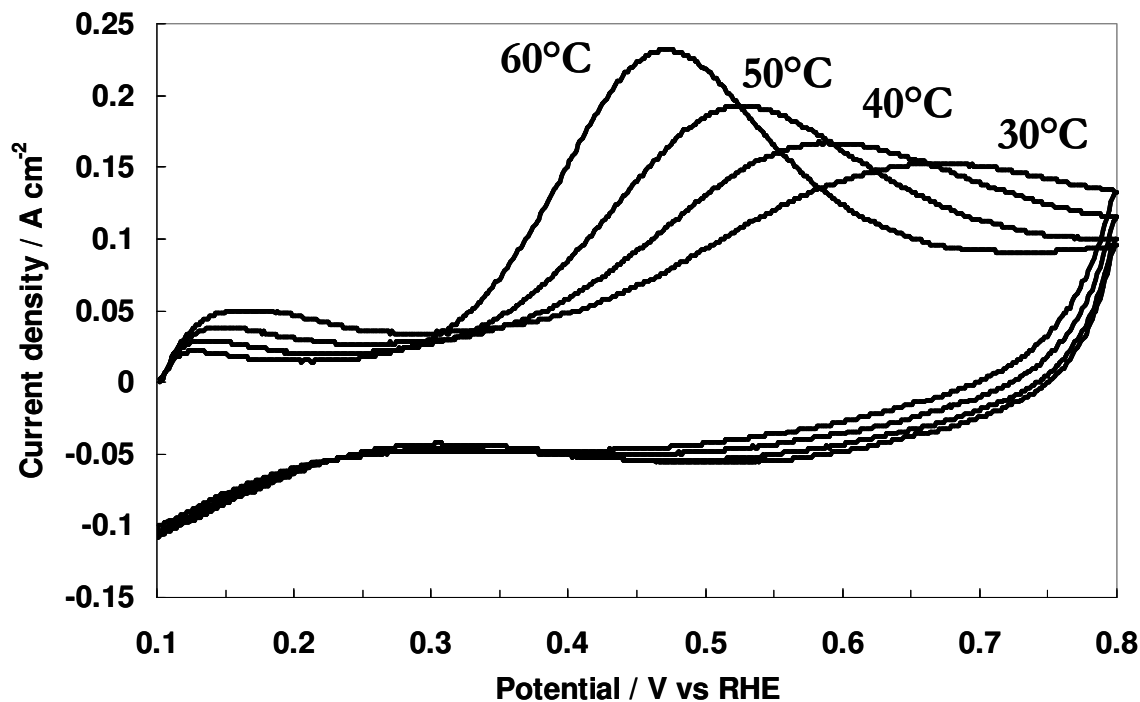


Figure 9. In-situ adsorbed methanolic residues stripping voltammetry at 85% Pt-Ru/C | Nafion 117 membrane interface in the presence of 5 mg cm⁻² Pt loading at different temperatures under the DMFC configuration.

behaviour for the cell equipped with $5 \text{ mg}\cdot\text{cm}^{-2}$ Pt loading on both anode and cathode compartments under ambient pressure. The power density increases from 32 to $75 \text{ mW}\cdot\text{cm}^{-2}$ passing from 30°C to 60°C , indicating the strong activation nature of the methanol electro-oxidation reaction. This is confirmed by the adsorbed methanolic residues stripping analysis carried out at various temperatures (Figure 9). Integrated charge and stripping potential provide information on the number and strength of the adsorbed species which participate to the rate determining step for methanol oxidation. The onset potential for the stripping of methanolic residues increases from 0.3 to 0.4 V as the temperature decreases from 60°C to 30°C (Figure 9). It appears that at 30°C the methanol adsorption does not reach a complete coverage at 0.1 V, whereas the coverage increases with temperature as reflected by the decrease of the hydrogen desorption peaks at low potentials. The stripping peak appears more sharp and increases in intensity as well as it shifts to lower potentials at higher temperatures reflecting faster desorption kinetics. Assuming that the methanolic residues are CO-like species and that the coverage at 60°C is approaching the monolayer ($\theta = 1$), the electrochemical active surface area of the anode catalyst is about $36 \text{ m}^2/\text{g}$ when the Pt loading is $5 \text{ mg}\cdot\text{cm}^{-2}$.

4. CONCLUSIONS

The influence of noble metal loading and catalyst utilisation on the electrochemical behaviour of low temperature (30°C - 60°C) DMFCs was investigated by steady-state polarisations and adsorbed methanolic residues stripping voltammetry. From these analyses, $5 \text{ mg}\cdot\text{cm}^{-2}$ seems to be the most suitable Pt loading for low temperature DMFC application. The maximum power density increased from 30 to 75 mW cm^{-2} at 60°C passing from 1 to $5 \text{ mg}\cdot\text{cm}^{-2}$ Pt loading on both anode and cathode at ambient pressure; whereas, only a slight increase was observed with $10 \text{ mg}\cdot\text{cm}^{-2}$, due to the decrease of catalyst utilisation.

ACKNOWLEDGEMENTS

The authors gratefully acknowledge the financial support of the European Commission through the Morepower Project SES6-CT-2003-502652.

References

1. M. Neergat, D. Leveratto, U. Stimming, *Fuel Cells*, 2 (2002) 25.
2. A.S. Aricò, P. Bruce, B. Scrosati, J.-M. Tarascon, W. Van Schalkwijk, *Nature Mat.*, 4 (2005) 366.
3. A. Blum, T. Duvdani, M. Philosoph, N. Rudoy, E. Peled, *J. Power Sources*, 117 (2003) 22.
4. M.A. Navarra, S. Panero, B. Scrosati, *Electrochem. Solid-State Lett.*, 8 (2005) A324.
5. R. Dillon, S. Srinivasan, A.S. Aricò, V. Antonucci, *J. Power Sources*, 127 (2004) 112.
6. X. Ren, P. Zelenay, S. Thomas, J. Davey, S. Gottesfeld, *J. Power Sources*, 86 (2000) 111.
7. S.C. Kelley, G.A. Deluga, W.H. Smyrl, *Electrochem. Solid-State Lett.*, 3 (2000) 407.
8. A.K. Shukla, P.A. Christensen, A. Hamnett, M.P. Hogarth, *J. Power Sources*, 55 (1995) 87.
9. E. Antolini, J.R.C. Salgado, L.G.R.A. Santos, G. Garcia, E. A. Ticianelli, E. Pastor, E.R. Gonzales, *J. Appl. Electrochem.*, 36 (2006) 355
10. X. Ren, M.S. Wilson, S. Gottesfeld, *J. Electrochem. Soc.*, 143 (1996) L12.
11. L. Liu, C. Pu, R. Viswanathan, Q. Fan, R. Liu, E.S. Smotkin, *Electrochim. Acta*, 43 (1998) 3657.

12. A.S. Aricò, A.K. Shukla, K.M. el-Khatib, P. Cretì, V. Antonucci, *J. Appl. Electrochem.*, 29 (1999) 671.
13. H.G. Petrow, R.J. Allen, US Patent 3,992,331 (1976).
14. A.S. Aricò, V. Baglio, A. Di Blasi, E. Modica, P.L. Antonucci, V. Antonucci, *J. Electroanal. Chem.*, 557 (2003) 167.